Proceedings of the Seventh International Conference on
Railway Technology: Research, Development and Maintenance
Edited by: J. Pombo
Civil-Comp Conferences, Volume 15, Paper 6.1
Civil-Comp Press, Edinburgh, United Kingdom, 2026
ISSN: 2753-3239, doi: 10.4203/ccc.15.6.1

Thermal Stress Analysis of CWR Switches: Influence of Switch Angle, Sleeper Type, and Rail Profile

J.-F. Ferellec and C. Eychene

SNCF Réseau,
France

Abstract

Continuous Welded Rail (CWR) tracks develop significant axial forces when subjected to temperature variations, and these forces can be amplified in the vicinity of switches due to their geometric discontinuities and heterogeneous support conditions. This paper presents an extended nonlinear finite element study aimed at quantifying thermal stress amplification in switches integrated into CWR zones. The model incorporates the full three-dimensional geometry of the switch, including the transition from common to separate sleepers, the detailed crossing region, and nonlinear longitudinal and lateral ballast resistances. A comprehensive simulation campaign is carried out to evaluate the combined influence of three key parameters: the switch angle, which determines the sleeper topology; the rail profile; and the sleeper type (timber or concrete), which affects the mobilised ballast resistance. For each configuration, the model computes the maximum axial stress induced during a temperature rise, relative to an equivalent straight CWR track. The results are synthesised into an engineering abacus that provides the peak axial stress as a function of temperature variation for any combination of switch angle, rail profile, and sleeper type. This abacus is intended to support railway engineers in assessing buckling risk, planning maintenance operations, and optimising neutral temperature management in switches installed on CWR tracks. The study demonstrates that switch angle, rail stiffness, and sleeper material all exert a significant influence on thermal stress amplification, and that their combined effect must be accounted for in engineering assessments.

Keywords: ballast track, continuous welded rail, switches & crossings, rail stress, simulation, FEM

1 Introduction

Continuous Welded Rail (CWR) tracks are widely used in modern railway networks because they provide improved ride quality and meet the performance requirements of high-speed lines. However, their continuous structure makes them particularly sensitive to temperature variations. When the rail temperature deviates from its neutral temperature, significant axial forces develop due to the rail–sleeper connection and the anchorage provided by the ballast. Excessive compressive forces may lead to lateral track buckling, while excessive tensile forces may result in rail breakage.

Traditional engineering methods, based on simplified analytical approaches or empirical rules, generally allow for a satisfactory evaluation of the thermal behaviour of straight CWR tracks [1:4]. In contrast, these methods rapidly reach their limits when applied to turnouts and switches, where the geometry is complex and the distribution of support conditions varies significantly. In such areas, the main and diverging rails may rest on the same sleepers, creating additional mechanical coupling that can locally amplify the stresses generated during thermal expansion.

Another important factor influencing the thermal response is the type of sleeper used in the switch. Concrete sleepers provide a much stiffer longitudinal and lateral support than timber sleepers, resulting in stronger mechanical coupling between the rails and increased transmission of axial forces. Timber sleepers, by contrast, offer more flexibility and damping, leading to lower effective longitudinal restraint. As a result, the sleeper type directly affects the magnitude and localisation of thermal stresses within the switch.

Previous work introduced a nonlinear Finite Element Model (FEM) developed to analyse the behaviour of CWR tracks subjected to temperature increases [5:8]. This model successfully reproduced characteristic phenomena such as breathing zones, the development of axial forces, and the onset of buckling under alignment defects.

The present paper extends this study to a comprehensive set of switch configurations. The objective is to evaluate the combined influence of the switch angle, the associated sleeper topology, which is directly determined by this angle, the rail profile and the sleeper type (timber or concrete) on the maximum axial stress generated during a temperature rise.

All results are synthesised into an engineering abacus, enabling rapid estimation of the expected maximum axial stress for any given switch configuration and temperature variation. This abacus is intended as an operational tool for railway engineers, supporting buckling-risk assessment, maintenance planning, and the optimisation of CWR installation parameters in the vicinity of switches.

2 CWR track model including a switch

The numerical model used in this study is based on a nonlinear finite element formulation implemented in ANSYS Mechanical. The objective of the model is to reproduce the longitudinal and lateral mechanical behaviour of a CWR track subjected to temperature variations, including the complex interaction mechanisms occurring within switches. The track is represented using a combination of beam elements for the structural components and nonlinear spring elements for the rail–sleeper–ballast interfaces (fig.1). Switches require additional modelling refinements due to their geometric discontinuities and the presence of common sleepers supporting both the main and diverging tracks. An important aspect of this study is the explicit consideration of sleeper type, which significantly affects longitudinal and lateral stiffness. Both concrete and timber sleepers are accounted for in the model, with distinct stiffness and resistance characteristics.

Rails and sleepers are modelled using beam elements (BEAM188 in ANSYS), which provide a three-dimensional, two-node beam formulation capable of capturing axial deformation, torsion, bending about both axes. Material properties (Young's modulus, Poisson's ratio, density) correspond to standard steel rails and timber or reinforced concrete sleepers (see examples in tab.1). Concrete sleepers provide higher stiffness and greater longitudinal restraint, while wooden sleepers are more flexible and introduce lower longitudinal and lateral stiffness into the system. These differences are captured through their Young's modulus, density, cross-sectional inertia, and ballast interaction characteristics. The rail profile is incorporated in the cross-section definition, influencing the axial stiffness EA and bending stiffness EI, both of which play an important role in the thermal response of the track. Interface forces between rails, sleepers, and ballast are represented by non-linear springs (COMBIN39 in ANSYS) exhibiting perfectly elastic–plastic behaviour. These springs model: longitudinal fastener stiffness, lateral fastener stiffness, vertical rail-pad rotational stiffness, longitudinal ballast resistance, lateral ballast resistance and vertical ballast support. Each spring is defined by a maximum elastic force, a maximum elastic displacement, a linear elastic branch followed by a plastic branch. This formulation captures the characteristic resistance–displacement response of ballast and fasteners under thermal loading. Sleeper type influences these interface properties: concrete sleepers produce higher stiffness and resistance, whereas wooden sleepers yield lower stiffness and increased deformability, thereby altering how thermal forces are transmitted along the track.

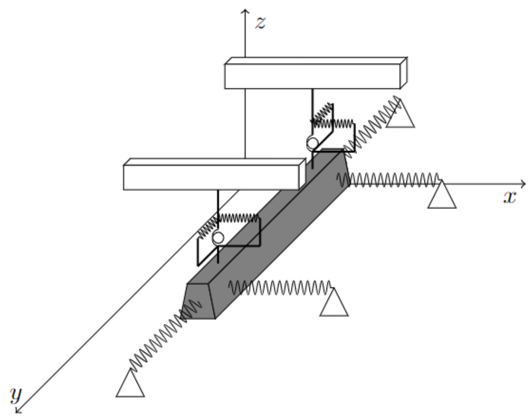

Figure 1: 1435mm gauge track model

Component	Property (unit)	Value
Rail (ex.)	*Young modulus E (MPa)*	2.1×10^5
	Poisson ratio	0.3
	Density (kg/m^3)	7860
	Section type 60E1 (mm^2)	7580
	Thermal expansion coefficient (mm/°C)	1.15×10^{-5}
Sleeper (ex.)	*Young modulus E (MPa)*	4.2×10^4
	Poisson ratio	0.25
	Density (kg/m^3)	1700
	Section type B440 (mm^2)	58300
	Length (m)	2.4
Fastener spring (ex.)	*Longitudinal maximum force (kN)*	16
	Longitudinal maximum elastic elongation (mm)	2
	Lateral maximum force (kN)	160
	Lateral maximum elastic elongation (mm)	2
Rail seat spring	*Vertical rotational elastic stiffness (N.mm/rad)*	4.5×10^8
Ballast/sleeper spring (ex.)	*Longitudinal maximum force (kN)*	20
	Longitudinal maximum elastic elongation (mm)	2
	Lateral maximum force (kN)	10
	Lateral maximum elastic elongation (mm)	2

Table 1: Parameters of the model

Switches introduce mechanical and geometric complexities that require special modelling considerations. At the beginning of the switch, the diverging track is close to the main track. Both tracks rest on the same sleepers, called common sleepers. These sleepers create a mechanical coupling between the rails, constraining their relative longitudinal displacement during thermal expansion. As the diverging track gradually separates from the main track, the distance between the two becomes large enough to justify the use of two separate sleepers, one for each track. The transition from common to separate sleepers—which depends directly on the switch angle θ—introduces a significant change in the local stiffness distribution. The switch angle θ dictates the rate at which the diverging track moves away from the main track, the number and position of common sleepers, the length of the transition zone, the mechanical coupling between the rails. A larger angle leads to a shorter zone of common sleepers, a sharper variation in track stiffness, more localised axial stress concentrations during thermal expansion. Thus, in this study, the switch angle is treated as a global parameter defining both the geometry and the sleeper topology.

The crossing area (frog) is a region of highly complex geometry involving changes in rail profile, gaps, and load-transfer mechanisms. To represent these effects accurately, the crossing is modelled using 3D volumetric element (SOLID185 in ANSYS). These elements provide full 3D stress representation, better capture of stiffness discontinuities, more realistic boundary conditions for the connected rail beam elements. Rails modelled as BEAM188 elements are coupled to the 3D crossing mesh using multi-point constraint equations ensuring both force and displacement compatibility.

A temperature rise ΔT is applied uniformly to the rails to represent thermal expansion. The analysis is purely static. Two solution strategies are used: Newton–Raphson iterations for configurations where no buckling is expected, Arc-length control for configurations susceptible to bifurcation or large lateral displacements. These strategies ensure convergence of the nonlinear system under varying stiffness conditions.

3 Model validation

Before applying the finite element model to switch configurations, a validation phase is carried out on a straight CWR track. This step ensures that the model can reproduce the well-known mechanical behaviour of continuous welded rails subjected to thermal loading, both in the longitudinal and lateral directions. The validation is based on two fundamental aspects: the development and redistribution of axial forces, the initiation of lateral instability (buckling) in the presence of alignment defects.

A 500-m-long straight track is modelled using the same elements and nonlinear interface laws described in Section 2. Both ends of the track are free to move longitudinally. A uniform temperature increase ΔT is applied to the rails. In the central region of the track, longitudinal restraint from fasteners and ballast prevents thermal expansion, generating an axial compressive stress that theoretically satisfies: $\sigma = E \, \alpha \, \Delta T$, where E is the rail Young modulus and α its coefficient of thermal expansion. The simulation reproduces this behaviour with excellent accuracy. When ΔT = 50 °C, the axial stress in the middle of the track matches the theoretical value. Near the free ends, however, the rails can expand which generates longitudinal displacements and a progressive reduction in axial stress. The regions where displacement is significant are known as breathing zones. The model predicts breathing zones approximately 100 m long on each side of the track — consistent with classical analytical expectations and field measurements. This confirms that the longitudinal behaviour of the CWR system is correctly captured.

A perfectly straight track exhibits no lateral deformation under uniform heating. To validate lateral response, a sinusoidal alignment defect, 15m long, 1mm large, is introduced at the centre of the track. When thermal compression increases, the initial defect amplifies and evolves into a characteristic damped sinusoidal deformation pattern, indicating the onset of lateral instability. The model successfully reproduces: the growth of lateral displacement with temperature, the bifurcation-type behaviour typical of rail buckling, the dependence of the instability threshold on defect amplitude. For increasing ΔT, the lateral deflection curve (fig.2) exhibits: a stable equilibrium, a limit point corresponding to the maximum ΔT_{max}, before loss of stability an unstable drop to a new configuration, a post-buckling stable equilibrium at ΔT_{min}. This sequence is consistent with classical nonlinear stability theory and with prior analytical and numerical studies of CWR buckling.

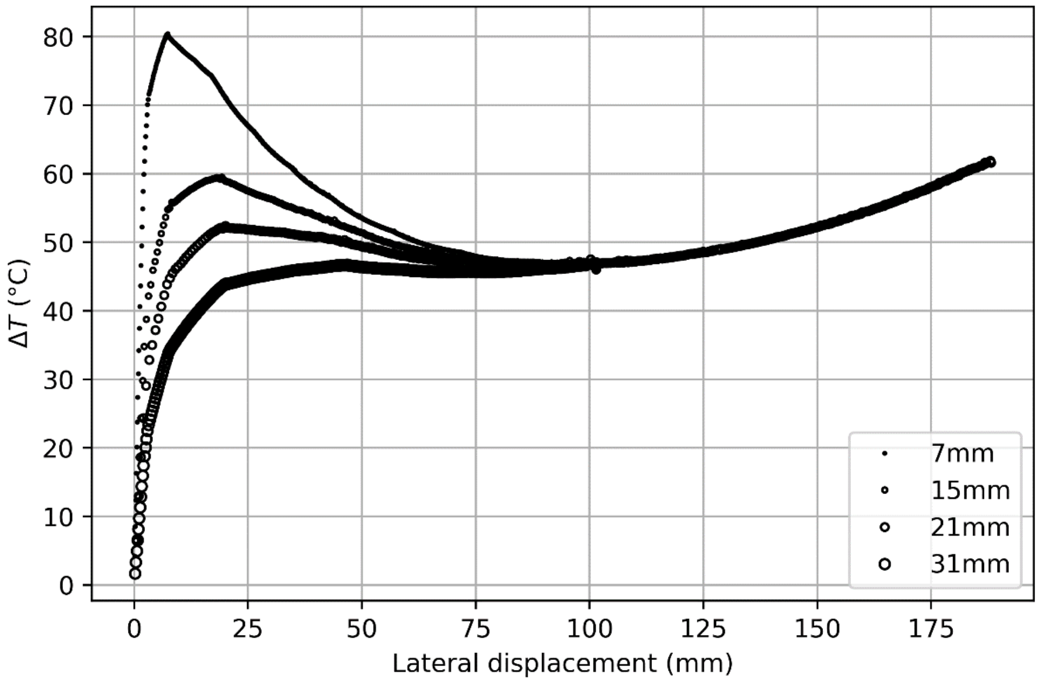

Figure 2: Relationship between temperature variation and lateral displacement of track middle

The validation simulations demonstrate that: the model accurately predicts axial force development in restrained rails, breathing zones and free-end displacements are realistic, lateral buckling mechanisms and bifurcation behaviour are correctly captured, the influence of alignment defects on stability thresholds is consistent with established literature. These results confirm that the model is suitable for analysing more complex railway systems, in particular switches, where geometric discontinuities and sleeper topology are expected to amplify local axial stresses. The next section applies the validated model to an extensive set of switch configurations to quantify the influence of switch angle, sleeper topology, and rail type on thermal stress amplification.

4 Simulation campaign for switch configurations

This section presents the systematic simulation campaign performed to evaluate the influence of three key parameters on the axial stress generated in railway switches subjected to thermal loading: the switch angle θ, the corresponding sleeper topology, intrinsically coupled with θ, the rail profile and the sleeper type (timber or concrete). The ballast resistance, longitudinal or lateral, depends on the type of sleeper. The objective is to quantify how these parameters influence the peak axial forces that develop during rail expansion. The resulting dataset forms the basis of an engineering abacus used to estimate thermal stresses in operational conditions.

The switch angle θ is the primary geometric parameter governing the divergence between the main and diverging tracks (fig.3). As the diverging track moves away from the main track, its support conditions transition from common sleepers (supporting four rails) to separate sleepers (one for each track). At the start of the switch, the two tracks are sufficiently close that both rest on the same sleepers. These common sleepers mechanically couple the longitudinal deformations of the two tracks, transfer axial forces from one track to the other, significantly constrain relative movements during thermal expansion. This coupling is responsible for high local rail axial stresses when temperature increases. As the diverging track progressively increases its lateral offset, a point is reached where common sleepers are no longer feasible. Beyond this point the rails are supported by separate sleepers, the mechanical coupling between tracks decreases sharply, longitudinal deformation becomes less constrained. The switch angle θ determines the number of common sleepers, the length of the shared-support zone, the location where the transition to separate sleepers occurs, the sharpness of the stiffness variation in the system. Small angles (e.g., 6°) lead to a large number of common sleepers, smoother geometric transitions, a more distributed stiffness gradient. Larger angles (e.g., 12°) result in a short common-sleeper zone, abrupt stiffness changes, stronger localized axial force concentrations. Because the sleeper topology is fully determined by the switch geometry, θ acts as a global parameter defining both the geometry and the structural support of the switch.

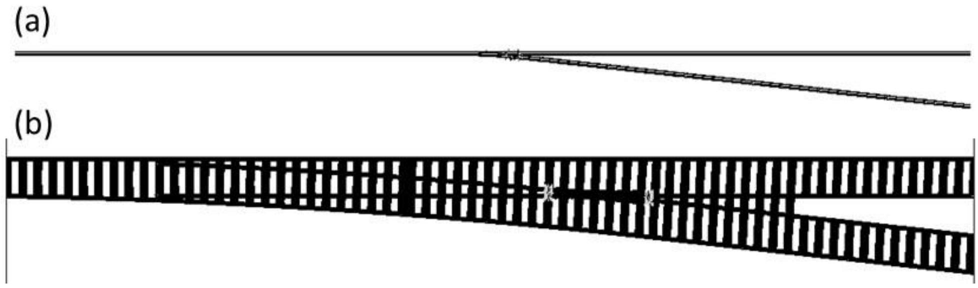

Figure 3: Switch model configuration: (a) global, (b) switch

In contrast to sleeper topology, the rail profile is an independent design parameter not dictated by the switch angle. The simulations consider several common profiles—such as 60E1 or 50E6—each characterized by distinct axial and bending stiffnesses. The rail profile influences thermal behaviour through the axial stiffness EA, which directly governs the thermal force generated by ΔT, the bending stiffness EI, which affects lateral stability and load transfer, the mass per unit length, which affects dynamic effects (although this study is static). A stiffer rail transmits higher axial forces through the common-sleeper zone, amplifying local stress peaks around stiffness discontinuities.

The type of sleeper (timber or concrete) also influences the thermal response through its interaction with the ballast. Timber and concrete sleepers do not mobilise the same levels of longitudinal and lateral resistance in the ballast layer. Concrete sleepers generally provide higher ballast resistance due to their greater mass, stiffness, and contact surface, resulting in stronger longitudinal and lateral restraint. Timber sleepers, being lighter and more flexible, mobilise lower ballast resistance values. These differences directly affect how thermal forces are transmitted along the switch and are therefore included as an independent parameter in the simulation campaign.

All simulations apply a uniform temperature increase ΔT, ranging from 0 to 100 °C, to the rails. Boundary conditions replicate a long CWR track: both track extremities are free to move longitudinally, no external lateral loads or transverse disturbances are applied, switch geometry and sleeper topology remain unchanged across simulations. The model therefore isolates the pure thermal response of the system, without train-induced forces or ballast degradation.

For each combination of (θ, rail profile, sleeper type, ΔT), the model records the axial stress along all the rails of the switch including its maximum σ_{peak}. This quantity is defined as the deviation from the axial stress that would develop in an equivalent straight CWR track for the same ΔT. It therefore represents the additional stress induced specifically by the presence of the switch. Figure 4 shows the axial stress along the four rail of the switch configuration of figure 3 with concrete sleepers and 60E1 rails. Stress peaks typically occur near the end of the common-sleeper zone, around the crossing, where geometric constraints are most pronounced, or at local discontinuities in stiffness or geometry. These peak values constitute the dataset used to construct the engineering abacus presented in Section 5.

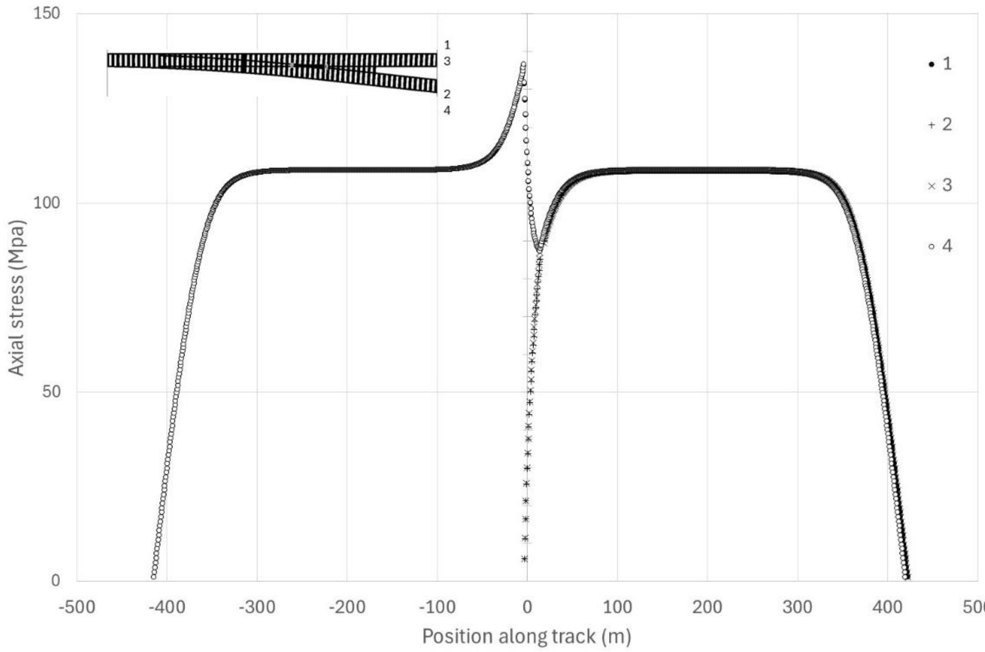

Figure 4: Axial stress along the four rails of the switch

5 Construction of the engineering abacus

The simulation campaign described in Section 4 yields an extensive dataset of peak axial stresses for different combinations of switch angle, sleeper topology, rail profile, sleeper material, and temperature rise. The purpose of this section is to synthesise these results into a practical engineering abacus that allows railway engineers to estimate, in a straightforward manner, the maximum axial stress generated in a switch for a given temperature variation. The abacus is built to be intuitive and field-ready, while directly leveraging the detailed nonlinear finite element results from the modelling effort.

Four parameters influence the peak axial stress σ_{peak} in the simulations: switch angle θ, sleeper topology (automatically determined by θ), rail profile, sleeper type (timber or concrete). Since sleeper topology depends solely on θ, the three independent variables controlling the abacus are ΔT (temperature variation), rail profile (e.g., 60E1, 50E6), sleeper type (timber or concrete). Thus, for each switch angle θ, a dedicated abacus page is created. Each page includes: x-axis=ΔT, y-axis=σ_{peak}; multiple curve families: one family per rail profile, within each family, two curves (timber and concrete sleepers). This structure preserves clarity while capturing all relevant variations.

For each simulation, the abacus reports: $\sigma_{peak}(\theta, \text{rail, sleeper type}, \Delta T)$. This quantity is defined as the excess stress produced by the switch relative to a straight CWR track subjected to the same temperature rise: $\sigma_{peak}=\max[\sigma_{switch}(\theta, \text{rail, sleeper type}, \Delta T)-\sigma_{straight}(\Delta T)]$. Because sleeper type influences stiffness and longitudinal restraint, it directly modifies σ_{peak}. Timber sleepers typically yield lower longitudinal stiffness and thus lower σ_{peak}, whereas concrete sleepers produce a stiffer support and higher axial force transmission.

The analysis reveals several robust trends across all angles θ, sleeper types, and rail profiles. For both wood and concrete sleepers, σ_{peak} increases almost linearly with ΔT up to 100 °C. This is expected because thermal force in a restrained rail is approximately proportional to ΔT if no buckling occurs. As described in Section 4, larger angles produce: shorter common-sleeper zones, sharper changes in support stiffness, and thus higher local stress concentrations. This effect is visible regardless of sleeper type. Sleeper material significantly affects σ_{peak}; concrete sleepers: stiffer longitudinal restraint, stronger coupling between the two rails, higher force transmission, higher σ_{peak} values; timber sleepers: more flexible and less stiff, partial relief of thermal forces, lower mechanical coupling, lower σ_{peak} values. This effect becomes especially relevant near the end of the common-sleeper zone. Rail axial stiffness EA magnifies stress: heavier profiles (60E1) lead to higher σ_{peak}, lighter profiles (50E6) lead to lower σ_{peak}. Across all configurations, peak stress consistently appears: at the transition between common and separate sleepers, and/or near the crossing, where rail constraints are highest.

For operational use, the abacus is designed to be simple and unambiguous. To use the abacus, the engineer must: identify the switch angle θ (from track documentation), identify the sleeper type, timber or concrete (can be inspected visually on site), identify the rail profile (marked on the rail web), measure rail temperature, compute $\Delta T=T_{rail}-T_{neutral}$, select the correct abacus page for the switch angle θ, locate the correct curve (rail profile, sleeper type), read σ_{peak} from the chart, compare σ_{peak} with buckling safety thresholds, define mitigation measures if needed (ballast reinforcement, neutral temperature correction, speed restrictions, etc.).

Because the abacus accounts for: geometric effects through θ, longitudinal stiffness effects via sleeper material, axial stiffness via rail profile, it can support: hot-weather operation planning, neutral temperature verification, maintenance prioritisation, switch design and optimisation. The abacus provides a refined, simulation-based assessment that complements and improves upon empirical rules traditionally used in CWR engineering.

6 Procedure for using the abacus

To apply the abacus in practice, engineers should follow the steps within table 2.

Step	Objective	Details
1	Identify the switch geometry	Retrieve the switch angle θ from: track layout drawings, asset management databases, markings present on the switch. This angle fully determines the sleeper topology (common vs. separate sleepers).
2	Identify the rail profile	Rail type (e.g., 60E1, 50E6) can be confirmed: from rail web markings, from maintenance records, or from design documentation.
3	Identify the sleeper type	Determine whether the switch uses: concrete sleepers, timber sleepers, or a mixed configuration (if applicable to your network). Sleeper type affects longitudinal stiffness and thus modifies σ_{peak}.
4	Determine the temperature rise ΔT	Measure: current rail temperature T_{rail}, neutral temperature $T_{neutral}$ (from stress-free measurement data or historical records). Then compute: $\Delta T = T_{rail} - T_{neutral}$.
5	Select the correct abacus page	Choose the page corresponding to the switch angle θ.
6	Locate the correct curve family	For the chosen θ: choose the curve for the correct rail profile, within that family select the curve for the appropriate sleeper type.
7	Read σ_{peak}	From the intersection with ΔT on the X-axis, read the corresponding value of σ_{peak} on the Y-axis.
8	Compare with allowable limits	Compare σ_{peak} with: internal safety limits, regulatory buckling thresholds, engineering guidelines for thermal stress. This step determines whether intervention is required.

Table 2: Procedure for using the abacus

The value of σ_{peak} obtained from the abacus helps guide decisions such as:
- Neutral temperature management. If σ_{peak} becomes too high for expected summer temperatures, engineers may adjust the rail neutral temperature by de-stressing, plan corrective works during moderate weather windows.
- Ballast reinforcement or renewal. High σ_{peak} often coincides with zones where ballast performance is critical. Actions may include: ballast tamping and stabilisation, ballast cleaning, shoulder reinforcement, crib compaction.
- Sleeper replacement or upgrade. Because sleeper type strongly affects σ_{peak}: replacing degraded timber sleepers with concrete ones, or replacing cracked concrete sleepers, can modify stress distribution and reduce risk.
- Operational restrictions. When immediate intervention is not possible, operational measures may be applied: speed restrictions, increased monitoring, temperature-dependent surveillance.

The abacus can support: hot-weather monitoring plans, CWR inspection protocols, identification of high-risk switches for prioritised patrols, deployment of trackside temperature sensors at critical locations. Switches with: large angles, concrete sleepers, heavy rail types, or known ballast issues, will rank higher in thermal risk.

The abacus can be integrated into: digital asset management platforms, maintenance decision support systems, switch condition monitoring software, engineering guidelines. By incorporating the simulation-based relationships between ΔT, geometry, rail profile, and sleeper type, the abacus enhances existing tools used for: network-wide risk mapping, predictive maintenance strategies, long-term infrastructure planning.

This section demonstrated how the abacus: provides a rapid, reliable estimate of the maximum axial stress in a switch, incorporates all critical physical parameters (θ, rail type, sleeper type), supports engineering judgement and operational safety, assists in maintenance and risk-management decisions during periods of high thermal loading. The next section concludes the study and outlines the contributions and future work.

6 Conclusions and perspectives

This study presents an extended numerical investigation of the thermal behaviour of Continuous Welded Rail (CWR) tracks incorporating railway switches. Building on a previously validated nonlinear finite element model, the analysis explores a comprehensive range of switch configurations to quantify the amplification of axial stresses generated during temperature rises. The main contributions of this work are as follows:

- A unified FEM model for track and switch systems. The model accurately reproduces fundamental CWR behaviours, including the development of axial forces, breathing zones, stiffness-driven stress concentrations, and the onset of lateral instability. It incorporates realistic support conditions through nonlinear ballast and fastener representations, and a detailed 3D description of the crossing.
- A systematic investigation of key parameters. Simulations were performed for combinations of switch angle θ, associated sleeper topology (determined directly by θ), rail profile, sleeper type (timber or concrete). This enabled the identification of the most influential structural factors governing thermal stress amplification.
- Detailed characterisation of axial stress peaks. Results show that localised increases in axial stress typically occur near the transition between common and separate sleepers, and the crossing, where geometric and mechanical constraints are strongest. Stress levels increase almost linearly with ΔT and are significantly affected by rail stiffness and sleeper material.
- Development of an engineering abacus. The simulation results have been synthesised into a practical abacus enabling engineers to estimate the maximum axial stress in a switch for any temperature rise. The abacus accounts for temperature variation, switch angle, sleeper type, rail profile. It is intended as a field-ready tool for maintenance planning, risk assessment, and operational decision-making.

Looking forward, several avenues can further enhance this work:

- Experimental validation. Field measurements on selected switches under varying thermal conditions will provide quantitative validation of the model and enable refinement of ballast and fastener parameters.
- Modelling of degraded track conditions. Introducing hanging sleepers, ballast fouling, or reduced lateral or longitudinal resistance will extend the abacus to real-world degradation scenarios.
- Extension to more complex switch types. Future work may include double-slip switches, crossovers, or high-speed turnouts with more complex geometric layouts.
- Dynamic and seasonal effects. Incorporating cyclic temperature loading or train-induced dynamic forces could improve the prediction of fatigue-related behaviour and long-term stiffness evolution.
- Digital integration. Embedding the abacus in engineering tools and asset-management platforms would support automated risk mapping across the network.

Overall, the methodology and results presented in this study contribute to a more accurate and operationally relevant understanding of thermal behaviour in switches installed on CWR tracks. The abacus offers a practical means for engineers to quantify thermal stress amplification and to implement maintenance strategies that enhance the safety and reliability of railway operations.

References

[1] A. Kerr, “An Analysis of Thermal Track Buckling in the Lateral Plane”, Report FRA-OR&D-76-285, Princeton University, Dpt of Civil Engineering, 1976.

[2] A. Kish, G. Samavedam, “Dynamic Buckling of Continuous Welded Rail Track: Theory, Tests, and Safety Concepts”, Transportation Research Records 1289, 1991.

[3] C. Esveld, “Improved Knowledge or CWR Track”, TU Delft, 1992.

[4] C. Esveld, “A Better Understanding of Continuous Welded Rail Track”, Rail Engineering International Edition Number 4, 1996.

[5] N-H. Lim, N-H. Park, Y-J. Kang, “Stability of Continuous Welded Rail Track”, Computers and Structures 81, 2219-2236, 2003.

[6] N-H. Lim, S-Y. Han, T-H. Han, Y-J. Kang, Parametric Study on Stability of continuous Welded Rail Track – Ballast Resistance and Track Irregularity, Steel Structures 8, 171-181, 2008.

[7] G.P. Pucillo, “Thermal Buckling and Post-Buckling Behaviour of continuous Welded Rail Track”, Vehicle system Dynamics, 54:12, 1785-1807, 2016.

[8] J.-F. Ferellec, T. Haljouji, B. Jeanselme, Z. Wang, M. Wone, “Modelling of CWR tracks including a switch”, Conference Railways, Prague, 2024.